PFC/JA81-11

A Tandem Mirror with Axisymmetric Central Cell Ion Confinement

J. Kesner, B.D. McVey,
R.S. Post, D.K. Smith

May 1981

Richard S. Post

NW21-205

Massachusetts Insitute of Technology

U.S. DOE Contract DE-AC02-78ET-51013

May 1981

Abstract

We discuss the ramifications of a tandem mirror design that provides axisymmetric central cell ion confinement. Such a design has the promise of eliminating central cell "neoclassical" and resonant cross-field transport as well as reducing the technology requirements for high field high-mirror ratio plugs. Microstability in plug and anchor can accrue from the use of "sloshing-ions" and MHD stability results from the use of an "outboard" minimum-B cell known as an anchor. Central cell parameters are obtained through the use of Ion Cyclotron Resonance Heating (ICRH) and an ICRH based startup scenario is proposed.

A number of adverse effects including enhanced crossfield transport, and increased sensitivity to field errors as well as increased complexity in fabrication and shielding of reactor size components derive from the non-axisymmetric quadrupole nature of MHD anchors that bound the central cell of a tandem mirror. Clearly a significant gain would be obtained from an axisymmetric confinement scheme.

In the original tandem mirror concept [1,2] and initial experiments the tandem mirror central cell was bounded by a minimum-B cell of very high energy density. These cells serve the dual function of MHD anchor for the system and electrostatic plug for ions. The thermal barrier concept [3] introduced in 1979 allowed for a substantial reduction in the end plug pressure at the cost of adding an additional mirror cell between the central cell and end plug and providing auxiliary electron heating and ion pumping.

There has recently been renewed interest in creating a sloshing-ion distribution in a mirror confined plasma as a means of combining the thermal barrier and ion plug into one, low-β mirror cell [4-5]. Sloshing ion distributions in low mirror ratio cells have been observed experimentally [6]. Such a sloshing-ion cell has the additional advantage of being able to electrostatically confine warm ions necessary for microstability. [7] Use of an "outboard" sloshing-ion plug has been explored and the concept developed for the proposed MFTF-B experiment. We have explored what has turned out to be a complimentary approach; use of an "inside" axisymmetric sloshing-ion plug adjoining the central cell [8]. MHD stability to flute and ballooning modes would derive from the use of an outboard minimum-B cell known as an "anchor".

The only requirement on this cell is the maintenance of a high beta plasma in a good curvature region. We have found that the most direct approach to MHD stability would employ neutral-beam heated anchors. The outboard anchor has the additional benefit of reducing the potential drop within the plug, thereby enhancing plug confinement and stability. Several other operating modes including a "hot-electron" anchor [8] and a "sloshing-electron" plug [9] are compatible with this geometry [8], but will be reported on elsewhere.

During the last year it has become evident that there are a great many end plug configurations that may be utilized in a tandem mirror device. While these configurations all rely on the same basic physics, each has its unique advantages (and disadvantages). The configuration that we have chosen is a particularly versatile one. Plug axisymmetry permits a variable mirror ratio and good neutral beam access to either perpendicular or off-perpendicular injection. The separation of the plug and anchor allows an independent variation of respective plasma parameters permitting an optimization of anchor parameters.

Use of RF and in particular ion heating in the ion cyclotron frequency range (ICRF) plays a key role in the operating modes described herein. ICRF provides the simplest means for heating the central cell to test scaling of beta limits and ultimately to heat a tandem reactor to ignition. Additionally we propose a startup scenario that utilizes ICRF both for central cell heating and for trapping the central cell efflux in the anchor and plugs.

Section II will discuss plasma parameters which form the basis of a design presented in Ref. [8] for the TARA experiment. Section III will describe the plug, and Section IV the anchor physics. Section V describes the central cell power balance and ICRF heating. Section VI describes startup of tandem operation.

II. Tandem Mirror Arrangement

The schematic arrangement is shown in Fig. 1. The central cell is bounded at both ends by a deep axisymmetric mirror cell formed between two high field coils. This mirror cell will form the sloshing-ion axisymmetric "plug" and will contain both the electron thermal barrier (at its midplane) and the ion plugging potential peak. The plug then maps through a transition section into a quadrupole minimum-B cell which acts as an MHD anchor to establish overall $\int p_{\parallel} \, d\ell/B$ stability. Since all ions confined in the central cell will either reflect from the high magnet field bounding the central cell or the potential peak within the sloshing-ion cell, they will not sample the quadrupole fields of the anchor and so their particle drifts are characteristic of a linear axisymmetric magnetic configuration. (We assume that the anchor is designed so that quadrupole currents required for equilibrium close within the anchor and do not upset the axisymmetry of the central cell and plug).

The plug forms in a mirror cell in which neutral beams are injected through the midplane at close to the loss cone angle so as to form an ion density (and potential) profile that peaks near the mirror throats and exhibits a minimum at the cell midplane. The predominant charge-exchange ionization of the neutral beams serves to maintain the sloshing character of the ion distribution function as well as to pump the central cell ions that trap in the potential well that forms at the plug midplane. ECRH can be employed to increase the midplane potential dip sufficiently to create a thermal barrier by maintaining a hot, magnetically trapped electron population. Electron heating is also used to heat and therefore expel electrons that trap in the off-midplane potential maxima, creating a sufficient potential peak to plug central cell ions. Obtaining the desired ion density profile in the plug requires a high mirror-ratio cell. Moreover, sufficient neutral beam and ECRH power for fueling, pumping and electron heating are required.

The high plug mirror ratio desired for confinement of the sloshing ions is easily obtained in axisymmetric cell. The high mirror ratio has the added advantage of reducing the flow of central cell ions that enter and trap in the plug which results in reduced pumping requirements.

The plug design proceeds from the need to confine a sufficiently hot central cell plasma to allow for the study of collisionless transport in the tandem central cell. Table 1 lists the parameters we have chosen in this study. They include central cell electron and ion temperatures of $T_{ec} = T_{ic} =$ 400 eV, a density of $N_c = 4 \times 10^{12}$ cm $^{-3}$ and $n\tau \sim 2.6 \times 10^{11}$ cm^{-3} - sec. We will later calculate the auxilliary power necessary to sustain these plasma parameters.

As described in the TMX-upgrade proposal [11], several parameters are important to produce a central cell plasma adequate for radial confinement studies. These may be listed as follows:

1) $\nu_c \, t_{\parallel} \approx (L_c/\text{mfp})$, the collisionality parameter for radial transport. We estimate $\nu_c \, t_{\parallel} \sim .013$ which indicates radial transport is collisionless.

2) $(\nu_c \, t_{\parallel}) \, (T_{ic}/\delta\phi_c) \, (B_m/B_c)$, the collisionality parameter for axial confinement. We estimate this parameter to be 0.09. This parameter being less than 1 indicates axial confinement is determined by the Pastukov scaling formula.

3) $\Delta\psi$, the azimuthal drift of an ion in one axial transit = $L_c a_i / r_c^2$ for L_c the central cell length, a_i the ion larmor radius and r_c the plasma radius. For our parameters $\Delta\psi \sim 3.6$. Thus we are operating in a sufficiently collisionless regime that non-axisymmetric tandems would exhibit resonant transport.

III. Sloshing-Ion Axisymmetric Plug

III-A. Ion Physics

The plug provides both the central cell ion plugging potential as well as the electron thermal barrier. In order to have a large off-midplane sloshing-ion density peaking a deep mirror well is required and we have chosen to use a mirror ratio of up to R = 6. Furthermore, we choose a minimum magnetic field of 5.0 kG which yields a 2nd harmonic ECRH frequency of 28 GC, a frequency where commercial gyrotrons are available. Neutral beams are injected at 35^{o} to the field direction. An axisymmetric cell of 2 m length (throat to throat) appears to be desirable from the standpoint of adiabaticity. Use of 4 coils to form the mirror cell (Fig. 1) permits good neutral beam access, reduces field power and permits a variable plug mirror ratio.

The detailed ion distribution function which results from neutral beam injection has been determined using a bounce-averaged Fokker-Planck code [12]. To simulate the presence of central cell plasma this code includes the so-called "left-hand boundary" [13].

This option assumes the presence at the plug midplane of a "passing" or "streaming" density at a prescribed level, N_s (b). The streaming plasma will reflect from the high potential peak that develops between the cell midplane and outer or right-hand mirror but can pass through the inner or "left-hand" mirror to circulate in the central cell. (The code only treats the right hand half of the plug).

We expect the outer potential to peak higher than a Boltzmann factor would predict due to the presence in the thermal barrier of "hot" magnetically trapped electrons. The peak to midplane potential $\delta\phi_a$ is approximated by

$$\delta\phi_a \sim T_{ew} \ln \left[\frac{N(a)}{F_{ec}\, N(b)} \sqrt{\frac{T_{ec}}{T_{ew}}} \right] \qquad (1)$$

which is the Fokker-Planck solution of Cohen et. al. [14]. T_{ew} is the warm electron temperature on the outside of the thermal barrier located at the cell midplane, b, T_{ec} is the central cell electron temperature, F_{ec} is the fraction of the density at b which consists of "cold" central cell electrons and N(a) (N (b)) is the total density at the peak potential (thermal barrier) point. To account for the presence of hot electrons we will use a modified Boltzmann factor to model the axial potential dependence:

$$\phi(z) - \phi(b) = C_1\, T_{ew} \ln(N(z)/N(b)) \qquad (2)$$

which requires that

$$C_1 = 1 + \frac{1}{2} \ln \left[T_{ec}/T_{ew}\, F_{ec}^{\,2} \right] / \ln(N_a/N_b). \qquad (3)$$

Results from a series of Fokker Planck runs for injection into a R = 6 mirror are shown in Table 2. The total midplane density including trapped and passing ions varies from 10^{12} up to 10^{13} cm^{-3}. Fig. 2 shows $f(v_\perp)$ and $f(v_{||})$ respectively for 35° injection at the midplane. Since ~ 30% of the ions are either of the trapped or streaming species, the distribution is expected to be stable to loss cone microinstabilities. (See discussion in Ref. 5). Additionally, the ratio of trapped + streaming density to streaming density, g_b, [$g_b \equiv (N_s(b) + N_t(b))/N_s(b)$], is ~ 6. ($g_b \gtrsim 3$ usually indicates two-stream acoustic stability. [5, 17].) Fig. 3 shows the density profile between the midplane and outer mirror.

The calculations shown in Table 2 indicate that as the injection angle approaches the loss cone angle, ion confinement decreases while charge-exchange pumping and therefore the tolerable central cell density level will increase. For 30° injection (T31, Table 2) a fixed mirror ratio of R = 6 (loss cone angle = 24°) and 110 Amperes injected we find a resulting mid-plane plug density of 2.3×10^{12} cm^{-3} and adequate pumping to support a central cell density of 8.5×10^{12} cm^{-3}. On the other hand (run T32), 35° injection would increase plug $n\tau$ by a factor of 3.5 so that a midplane density of $9.5 \times 10^{12} cm^{-3}$ would result from 110 Ampere injection and $4.2 \times 10^{12} cm^{-3}$ would result from 60 A injection (T36). Reducing the neutral beam current to take advantage of the increased $n\tau$ however, gives a proportionally smaller charge-exchange pumping current and the maximum allowable central cell density for run T36 is accordingly reduced to 4×10^{12} cm^{-3}. Additionally, we have seen in these calculations that injection very near to the loss-cone (i.e. 30° injection) can lead to a discontinuity in the resulting potential profile, that is, to sheath formation within the cell as predicted by idealized models for strongly pumped thermal barriers [15, 16]. This effect is not observed in the 35° injection runs.

In the proposed experiment we would fix the injection angle but have the ability to vary the loss cone angle (by changing the plug mirror ratio) as a means of adjusting the relative pump strength. We choose a base case injection angle of 35° at a mirror ratio of R.6 corresponding to run T36 (Table 2). The ability to vary the plug mirror ratio derives from the use of 4 coils to form each plug. Thus, without providing extra neutral beam modules, we will have a control knob on the pumping to fueling ratio.

Results of Fokker-Planck runs also indicate that if a larger warm plasma

trapping rate were to occur in the plug this could be compensated for by a reduction in central cell density.

III-B. Electron Physics

We will now use the densities and potentials obtained for 35° injection R = 6 to calculate paramenters related to the electron physics of the plug and anchor.

The determination of electron parameters follows closely the methods outlined by Logan in the Physics Basis for MFTF-B (4). We will use a similar notation to this reference. Three electron species are assumed to be present in this cell: "cold" central cell electrons of density $N_{ec}(z)$, magnetically trapped "hot" electrons $N_{eh}(z)$, and an electrostatically trapped "warm" species $N_{ew}(z)$. Three ion species are considered: central-cell passing ions of density $N_{ic}(z)$, magnetically trapped "sloshing-ions", $N_{ih}(z)$, and cold ions that trap in the potential well, $N_{it}(z)$. The total density at b will be written as N_b, etc. The relative densities of these ion species were determined from Fokker-Planck runs just described and we choose central cell parameters $T_{ec} = T_{ic} \Rightarrow 400$ eV, $N_c = 4.0 \times 10^{12}$ cm^{-3}. The experimental knobs are the ECRH power into the hot electrons (resonant at the plug midplane (b)), ECRH or other heating power into the warm electrons, and the electron source into the warm electron region (located outside of the thermal barrier at b). In the actual calculations of parameters, we

will choose the fraction of the midplane electron density that is due to cold electrons, F_{ec} the warm electron temperature T_{ew}, and the warm electron confining potential $\delta\phi_a$, and calculate the resulting requirements on pumping and heating.

The streaming ion density at b, $N_{ic}(b)$, can be approximated by [3]

$$N_{ic}(b) \simeq B_b/B_{max} \sqrt{T_{ic}/\pi\delta\phi_b}\ N_c. \qquad (4)$$

Defining F_{ec} as the ratio of central cell electrons at b to the total density at b

$$F_{ec} \equiv N_{ec}(b)/N_b$$

we can write the neutrality condition at b to be

$$N_{ec}\exp(-\delta\phi_b/T_{ec}) = F_{ec}\ N_i(b). \qquad (5)$$

N_b is determined by calculations ($4.2 \times 10^{12} cm^{-3}$) and we choose $F_{ec} = 3.2\%$. (This choice will be seen to follow from a hot electron particle balance and the restriction that the electron distribution remain monotonic.) $\delta\phi_b$ is the barrier potential ($\delta\phi_b = \phi_e - \phi_b$). Eqn. 5 then yields $\delta\phi_b/T_{ic} = 3.4$ or $\delta\phi_b = 1.4$ keV. We desire the central cell ion confining potential ($\delta\phi_c$) to be about twice the ion temperature and choosing $\delta\phi_c = 2 \times T_{ic} = 800$ eV ($\delta\phi_c = \phi_a - \phi_e$) we find $\delta\phi_a$ ($\equiv \phi_a - \phi_b$) to be $\delta\phi_a = 2.2$ keV.

For beams injected at an energy ($\bar{E}_{inj}$ = 10 Kev) and an injection angle of $\theta_{inj} = 35°$, the mirror ratio defining the bounce point $R_a = B_a/B_b$ is

$$R_a = (1 - \delta\phi_a/E_{inj})/\sin^2\theta_{inj} \approx 2.4 \qquad (6)$$

The Fokker-Planck peak sloshing ion density is found to be 1.1×10^{13} cm^{-3} and we take $N_{eh}(a) \sim 0.5\, N_{eh}(b) = 2.1 \times 10^{12}$ cm^{-3}. Neutrality then yields $N_{ew}(a) = 9.0 \times 10^{12}$ cm^{-3}.

We will now consider the variation of warm electron temperature, T_{ew}, as a function of electron current density J_e entering into the warm electron region from external sources. The electron particle balance between trapping of central cell or ionization source electrons and collisional loss, from the Fokker-Planck equation [14] gives the result:

$$J_e = N_{ew}(a)/\tau_{ew} \left[1 - \frac{N_{ec}(b)}{N_{ew}(a)} \sqrt{\frac{T_{ew}}{T_{ec}}} \exp\left(\delta\phi_a/T_{ew}\right)\right] \qquad (7)$$

with τ_{ew} the Pastukhov confinement time. For T_{ew} = 700 eV we find $n\tau_{ew} = 4.3 \times 10^{10} cm^{-3}$-sec and the electron current into a 10 ℓ volume is 1.65 A. For a fixed warm electron confining potential ($\delta\phi_a$) the larger the electron source (J_e) into this region, the higher must be the warm electron temperature so that these electrons boil out sufficiently quickly. Clearly, higher J_e requires increasing electron heating power.

The chosen value of T_{ew} is consistent with the criterion for stability of acoustic two-stream modes. (In order to have sufficient Landau damping to maintain stability Baldwin et al. [17] have found a requirement that $T_{ew} \lesssim 3.5\, T_{ic}$ or $T_{ew} < 1.4$ KeV.)

The maintenance of this electron temperature can be estimated by calculating the power required to expel the electrons which trap in the warm electron region. There exist two electron sources into this region; the cold electron source, J_e which was determined by Eqn. (7) to be 0.17 mA/cc and the trapping of central cell passing electrons in this region, J_{in}, which may be estimated from Ref. [5]

$$J_{in} = \frac{q\, n_{ec}(b)}{\tau_{ew}} \left(\frac{T_{ew}}{T_{ec}}\right)^{1/2} \exp(\delta\phi_a T_{ew}) \qquad (8)$$

to be 0.14 mA/cc. We can then estimate the power into the warm species following [5] to be 9.3 KW into a volume of 10 ℓ at T_{ew} = 700 eV. The power requirement would increase for higher electron temperature.

The parameter F_{ec} is determined by a hot electron particle balance which may be written as follows [5]

$$F_{ab} \frac{V_{ea}}{V_{eb}} (J_e + J_{in}) + J_{cb} \approx q \frac{(1-F_{ec})\, n_b^2}{2.4\times10^8\, E_{eh}^{3/2} \log_{10} Reff} \cdot \qquad (9)$$

The first term on the left side of the equation represents the fueling of the hot electron population by "warm" electrons that boil out of the potential well $\delta\phi_a$. F_{ab} is the fraction of these electrons that become magnetically trapped and V_{ea}, V_{eb} are the respective volumes occupied by the electrostatic and magnetically trapped species. J_{cb} represents the upward diffusion of the central cell electrons present at b.

$$J_{cb} \sim \frac{F_{ec}\, n_b^2}{2.4\times10^8\, T_{ec}(E_{eh})^{1/2} \exp\,(E_b'/T_{ec})} \qquad (10)$$

Where $E_b' = \delta\phi_b/(R-1)$, the minimum energy of magnetically confined electrons and E_{eh} is the hot electron mean energy. The right hand side of 10 represents the pitch angle scatter loss of these hot electrons. Setting E_{eh} = 12 keV and taking $F_{ab}\ V_{ea}/V_{eb} = 0.5$ we can solve 10 to get $F_{ec} \sim 3.2\%$. Additionally, since ECRH heats in a diffusive process we expect the electron distribution function to remain monotonic. This imposes a lower limit on F_{ec}

$$F_{ec} \gtrsim E_b'/E_{eh} = 0.023 \qquad (11)$$

If F_{ec} would drop below this level the loss rate of hot electrons would increase, preventing further increase in the hot electron population. We have chosen $F_{ec} = 0.032$ from the above analysis.

An estimate of the ECRH power necessary to maintain the hot electron species can be made according to [5]

$$P_{ECRH}(b) \sim \frac{(1 - F_{ec})\ N_b^{\,2}}{2.4 \times 10^8\ E_{eh}^{\,3/2}\ \log_{10} R_{eff}}\ (E_{e\ell} - T_{ec}) \qquad (12)$$

with $E_{e\ell}$ the mean loss energy. Estimating $E_{e\ell} \sim \frac{1}{2} E_{eh}$ yields 2.0 KW into a 10 ℓ volume. These parameters are listed in Table 3.

IV MHD Anchor

IV-1. Introduction

MHD stability is most simply obtained by connecting the plugs to high beta minimum-B cells which we shall call the outboard anchors located outside of the central cell-plug region. The most conservative approach is use of neutral beam driven quadrupole mirror cells as has been shown on TMX.

In this arrangement we connect the flux tube that exits the plugs to the anchor through a transition region. Within the transition section the circular flux tube leaving the plug is mapped into an ellipse where it joins to the anchor. A low-beta plasma present in the transition zone provides electrical connection between the anchor and plug and also can provide some stream and fueling for the anchor.

The critical problem in outboard-anchor operation is microstability. To provide for microstability we have developed a design in which the neutral beam ion sources establish a microstable ion distribution function; a sloshing-ion distribution with an approximately 10% fraction of cold electrostatically trapped plasma near the midplane. To accomplish this the neutral beams are injected at a 65° angle with respect to the machine axis in a mirror ratio = 2.5 cell. Use of a Yin-Yang coil set permits access at 45° to the symmetry planes which ameliorates the undesirable geometric effects that come from injecting in the plane in which field lines are fringing. Midplane injection provides pumping from the neutral beam charge-exchange and eliminates the need for additional pump beams.

A number of additional constraints must be satisfied in an outboard anchor arrangement. They are as follows:

1. High anchor beta; $\beta_a > 10\%$, required for ballooning stability for our desired central cell and plug beta's.
2. The peak anchor density, $n_a(c)$, should be below the peak plug warm electron density, $n_{ew}(a)$, if we desire to keep the anchor potential peak below that of the plug and thereby assure that all central cell ions are trapped in a purely axisymmetric region. Thus, $n_a(c) < n_{ew}(a) \approx 9 \times 10^{12} cm^{-3}$.
3. The minimum ion energy for confinement E_i^*, is determined by the potential drop between the potential peak and the outer mirror throat, $\delta\phi_c$ (see Figure 4). For R_c the mirror ratio relating the magnetic fields at the respective locations we get

$$E_i^* > \delta\phi_c/(R_c - 1) \sim 4.5 \text{ keV}$$

This value suggests use of 20 keV neutral beams to insure that the one-third energy component would be confined. (A degradation of central cell parameters would reduce $\delta\phi_c$ and thereby E_i^*).

4. Although the above three constraints require high ion energy for a given field level, this ratio is limited by adiabaticity requirements. We find this restriction to be approximately $E_i(\text{keV})/B^2(\text{KG}) \lesssim 1.9$ [8].

A set of parameters consistent with these constraints is shown in Table 4. Each anchor will utilize three 45A neutral beam modules to insure delivery of 100 A (atomic) within a 9 x 33 cm footprint (full width between 1/e points).

IV-2. Fokker-Planck Calculations

In order to obtain a significant midplane density depression (>20%) and not unacceptably degrade confinement we require a relatively high mirror ratio cell. Detailed Fokker-Planck studies have shown that the desired density dip and adequate confinement can be obtained with an anchor mirror ratio, of R_a = 2.5 and 65° midplane injection. No additional pump beams are required.

Input parameters for a series of runs are shown in Table 5. Results of these calculations are shown in Table 6. Comparison of run 42 with 39 indicates a considerable gain in midplane density depression accrues as a result of going from 70° to 65° injection. Furthermore, a comparison of runs 36 and 39 indicates that a sharp increase in confinement results from going from a mirror ratio of 2 to 2.5 in the calculation. The degree of safety offered for the mirror ratio = 2.5, 65° injection case is important because of geometric effects of the finite geometry on outer confined field lines.

Comparison of runs 39 and 43 shows the effect of increased neutral pressure which tends to both fill in the potential depression and to degrade high energy ion confinement. Examination of the resulting perpendicular and parallel ion distribution function for run 43 indicates that cold electrostatically trapped ions make up approximately 10% of the density.

IV - 3. Anchor Operation

We have assumed that a 10% fraction of cold trapped plasma is sufficient for microstability. This can be seen by application of the scaling law from

Baldwin and Jong [18].

$$n_{w/n_h} \approx \left[\rho_{i/R_p}\right]^{4/3} \quad \frac{\phi_m}{E_h(R-1)} \quad \left[L_p/L_s\right] \qquad (13)$$

with $n_h(cm^{-3})$ the hot plasma density, $n_w(cm^{-3})$ the warm electrostatically trapped component, ρ_i the ion gyroradius, R_p the plasma radius, ϕ_m the total potential drop in the mirror (midplane to mirror throat), (L_p/L_s the ratio of mirror length to stabilized region length, E_h the mean hot ion energy and R the mirror ratio. Taking E_h = 11 keV, L_p/L_s = 1.5, R = 2.5, R_p/ρ_i = 3, ϕ_m = 4.5 yields $n_w/n_h \sim 0.1$.

The physics of trapping of warm plasma in the local depression created by the hot sloshing-ions can be illustrated using a simple model. For a neutral density n_o ($n_o = 3.2 \times 10^{16} P_o(torr)$) the cold ion source ($cm^{-3}$) is given by

$$S_i = n_o[n_h(\langle\sigma v\rangle_{cx} + \langle\sigma v\rangle_i)_h + n_c\langle\sigma v\rangle_{ic}] \qquad (14)$$

with $\langle\sigma v\rangle_{cx}$ the charge exchange and $\langle\sigma v\rangle_i$ the total ionization rate coefficients. The dominant ionization term is charge-exchange on the hot-ions so that production of warm plasma adds an additional loss for the hot ions.

The loss rate for cold plasma from the local potential depression is due to Pastukhov-type collisional loss processes and to charge-exchange on the neutral beams and the latter process is seen to dominate. If the cold ions account for 10% of the total ion density then 10% of the neutral beam charge-exchange takes place on the cold ions. For example, the charge-exchanged current shown in Table 6 (#39) is about 2 A, so that the charge-

exchange pump on warm ions would be about 0.2A. The collisional loss of the warm ions can be shown to be ~80 mA [18]. Equation 14 can then be used to determine a required neutral density $7.0 \times 10^{8} cm^{-3}$ (for a 5 ℓ warm ion volume) to balance this loss rate.

Notice that an additonal hot ion source, charge-exchange of neutral beams on warm ions, approximately balances the added hot-ion loss caused by charge-exchange of hot ions on neutrals since source and loss rates for the warm component have to balance. Thus degredation of hot-ion confinement is not expected to accompany the warm ion production.

If we balance the cold neutral ionization rate ($\sim n_o n_h \langle \sigma v \rangle_{cx}$) with the charge-exchange pump rate of the cold plasma given by

$$J_{cx} \sim n_c \left(\frac{J_b}{e v_b} \right) \langle \sigma v \rangle_{cx} \tag{15}$$

for J_b the neutral beam current density (A/cm^2) and v_b(cm/sec) the beam velocity ($J_b/ev_b \equiv n_b(cm^{-3})$ the beam neutral density) we then find

$$n_o \sim \left(\frac{n_w}{n_h} \right) n_b . \tag{16}$$

Thus, the required neutral pressure is proportional to the neutral beam current density and the desired warm ion fraction. For a higher neutral pressure the warm density increases until the density depression fills in to the point that the Pastukhov loss becomes comparable to the neutral beam pump rate.

IV - 4. Transition Region Physics

The transition region density must be sufficient to maintain good electrical connection between the plug and anchor and should have low beta so as not to provide a significant drive for flute and ballooning. In the TARA design drift orbit pumping [19] will eliminate high energy ions which have unconfined vacuum field drifts whereas warm ions $E_i \lesssim T_e$ have confined drift orbits due to the dominant E ×B drift caused by the radial potential profile.

The warm ion density is determined from a balance of neutral gas ionization rate with Pastukhov loss over the potential barrier that develops in the transition region.

The ionization rate is given by

$$J_i = n_o n_t \langle\sigma v\rangle_e \quad \text{cm}^{-3}\ \text{sec}^{-1} \qquad (17)$$
$$= n_t^2/n\tau$$

for J_i the ionization current, n_o the neutral density, n_t the transition electron density, $\langle\sigma v\rangle_e$ the electron impact ionization rate coefficient and $n\tau$ the Pastukhov confinement time. Transition electrons equilibrate with the warm plug electrons at T_{ew}. If we choose the anchor density, n_a, and apply a Boltzmann relation for the transition density we obtain

$$n_{ot} = \frac{n_a}{\langle\sigma v\rangle_e (n\tau)_{ii}} \; T_i/\delta\phi_{ta} \exp\left[-\delta\phi_{ta}(1/T_{ew} - 1/T_i)\right]. \qquad (18)$$

T_i is determined by an ion energy balance which we will not solve here (the results are not sensitive to T_i). For T_i = 100 eV and $n_{ot} = 10^9$ cm^{-3} we obtain $\delta\phi_{ta}$ = 300 eV, and $n_t = 1.9 \times 10^{12}$ cm^{-3}. This corresponds to a current leaving the transition region of 0.64 A, approximately equal to the ionized current of the neutral beams. As the neutral pressure in the transition region is varied, the transition density, ion temperature and confining potential will adjust so that the outflow equals the source.

These parameters yield a transition beta of 0.007 for a transition B-field of 3kG.

IV - 5. MHD Ballooning Limits

The quadrupole end plugs of the TARA outboard anchor are minimum-B and support a high beta hot ion plasma. The potential instability of the central cell and axisymmetric plug due to their bad curvature are rendered

stable by connection to the anchors, provided the anchor beta, β_a, is sufficiently high.

MHD analysis has two basic focal points: stability of flute-type perturbations and of the finite $k_{\parallel}$ ballooning modes. The latter modes present more severe restrictions on the central cell pressure and therefore determine the peak central cell pressure that the system can support.

Kaiser has developed a computational solution to the ballooning analysis [20] which applies an energy principle valid in the large aspect ratio and short-perpendicular wavelength limit. The problem is solved in the vacuum field geometry including the long-thin mod-B finite-beta corrections.

Results of Kaiser's calculations for the TARA coil set are shown in Fig. 5 in which we show marginal stability limits for several values of anchor beta obtained by varying relative beta values in the plug and central cell. The curve for 13% anchor beta, the reference case, was extrapolated from the calculations. For 13% anchor beta and 3.5% axi-plug beta we obtain a peak central cell beta, β_c of $\beta_c \sim 5\%$. The actual operating point is shown by the square. For a higher anchor pressure the central cell and plug pressures could increase. We however expect that FLR corrections to the theory will permit considerably higher tandem beta for a fixed anchor pressure.

A typical ballooning mode eigenfunction for marginal stability is shown in Fig. 6. Notice that the eigenfunction tends to bend in the thin fan region adjoining the anchor where magnetic bending energy is minimal so as to peak up where the pressure-weighted bad curvature is maximum, at the central cell edge.

V. Central Cell Power Balance

In this section, we describe the particle and energy balance of the central cell consistent with the neutral beam parameters and ECRH power input assumed in the design of the sloshing ion cell. The starting point is the ion particle balance where the Pastukhov ion loss will be supplied by a cold gas feed.

$$I_{gas} = I^{i}_{LOSS} = \frac{q\, K_1 N_c^{\,2}\, V_c}{(N\tau)_{ic}} \qquad (19)$$

I_{gas} is assumed to be the ionized current provided by the cold gas feed. $K_1 \simeq .33$ is a density squared averaged profile parameter [11]. $V_c \simeq 153\ \ell$ is the effective volume of the central cell, and the ion confinement time is given by;

$$(N\tau)_{ic} \simeq 2.5 \times 10^{10}\, T_{ic}^{\,3/2} \left(\frac{A}{2}\right)^{1/2} g(R)\, \frac{\phi}{T_{ic}}\, e\left(\phi_c / T_{ic}\right) \qquad (20)$$

$$g(R) = \sqrt{\pi}\, \frac{2R+1}{4R}\, \ell n\,(4R+2)$$

Using the base case parameters $R = 7.5$, $\phi_c/T_{ic} = 2$, $A = 1$, $N_c = 4.0 \times 10^{12}\ cm^{-3}$ and $T_{ic} = .4$ KeV, we have

$$(N\tau)_c = 2.2 \times 10^{11}\ sec\ cm^{-3}$$

$$I^{i}_{LOSS} = I_{gas} - 0.58A$$

In calculating the ion particle loss, radial transport has been assumed negligible for the axisymmetric mode of operation.

The ion power balance has the form:

$$P_{ICRH} + P_{e \to i} = I^{i}_{LOSS} (\phi_c + T_{ic})$$

$$+ I_{gas} (1.5) T_{ic} \frac{\langle \sigma v \rangle_{cx}}{\langle \sigma v \rangle_{ion}} \qquad (21)$$

In Eqn. 21 we have allowed for auxiliary power input to the ions via ICRH. $P_{e \to i}$ is the energy transfer rate between electrons and ions given by;

$$P_{e \to i} = 4.8 \times 10^{-8} \, q \, K_1 \, V_c \frac{N_c^2}{T_e^{3/2}} (T_e - T_i) \, (W) \qquad (22)$$

For the reference case parameters $P_{e \to i} \sim 0$; however, we include this power term since the electron temperature may rise above the ion temperature dependent upon the fraction of warm and hot electrons that thermalize in the central cell.

The power loss terms in Eqn. 21 are from particle loss and from charge exchange on the cold gas feed. For the base case, $\langle \sigma v \rangle_{cx} / \langle \sigma v \rangle_{ion} \approx 2$, the total ion loss is,

$$P^{i}_{LOSS} \sim 1.3 \text{ KW}$$

This rather small ion power drain can be readily supplied via ICRH.

Ion heating can be accomplished in the central cell through the generation of electromagnetic wave modes in the plasma. Either the ion cyclotron, "slow" wave or the magnetosonic, "fast" wave modes may be excited and then damped by ion cyclotron absorption. In order to achieve efficient power transfer using the slow wave a very restrictive condition of matching the $k_{||}$ (parallel directed wavenumber) spectrum of the antenna structure with the $k_{||}$ of the wave mode must be satisfied. This matching implies the use of an antenna which excites a narrow $k_{||}$ range centered at a relatively large $k_{||}$, such as a Stix coil. Furthermore, for a given antenna proper k-matching will only be possible for a certain range of plasma density and diameter [21].

A more practical antenna design and efficient operation over a broad range of central cell parameters are obtained by relying on coupling to fast wave modes. The excited fast wave modes may be either propagating ($k_{||}^2 > 0$) or evanescent ($k_{||}^2 < 0$). In the latter case the wave fields exist essentially as the near fields of the antenna and do not propagate away from it. However, the polarization of the fast wave is retained. The near field case is relevant for the machine parameters used previously in this paper, whereas the propagating case will apply in larger machines. Damping of the fast waves is weak because they are almost right circularly polarized at $\omega = \omega_{ci}$. However, the weak damping can be offset by strong, efficient excitation resulting in effective ion heating. The effectiveness of this technique has been demonstrated in the Phaedrus end plug [22] and central cell [23] ICRH experiments. The well known technique of minority ion species heating circumvents the poor polarization of the fast wave at $\omega = \omega_c$ (majority) and provides another variation on fast wave heating in the central cell.

These techniques can be used for central cell heating as a means of testing radial transport scaling with ion temperature and ballooning limitations imposed on beta. Ultimately, ICRF can supply a means of heating the central cell to ignition in a reactor.

The ion particle loss is balanced by the loss rate of electrons which determines the confining potential (ϕ_e) of the central cell electrons.

$$\frac{q\ K\ N_c^2\ V_c}{(N\tau)_{ec}} = I^i_{LOSS} + 2\ I_b + 2\ I_e \qquad (23)$$

In the above equation, $I_b \sim 3A$ is the neutral beam ionization current in the sloshing ion cell, and I_e is the current source for the warm electrons due to neutral beam ionization. From Section III-B I_e is in the range of $\sim$ 1.7 A. The Pastukhov confinement time for the electrons is given by

$$(N\tau)_{ec} \sim 5.6 \times 10^8 \frac{g(R)}{2} T_{ec}^{3/2}\ \phi_e/T_{ec}\ e\left(\phi_e/T_{e_c}\right) \qquad (24)$$

Solving the last two equations for ϕ_e, we obtain, $\phi_e \sim 3\ T_{ec} \sim 1.2$ KeV.

The electron power balance has the following form:

$$P_{ECRH}^{b} + P_{ECRH}^{a} = P_{e \to i} + I_{LOSS}^{i} (\phi_e + T_{ec})$$

$$+ 2\, I_{sic} (\phi_e - \phi_b + T_{ec}) \qquad (25)$$

$$+ 2\, I_e (\phi_e + \phi_c + T_{ec})$$

The central cell electrons will be heated by the ECRH power used to heat both the warm and hot electrons, since these electrons thermalize in the central cell due to the positive overall confining potential with respect to ground. In the previous section, this power input was estimated to be ~ 7 KW. The terms contributing to electron power loss are the energy transfer to the ions, and the loss of potential and kinetic energy of electrons originating from ionization in the central cell, in the barrier cell and in the potential peak, respectively. The total loss is estimated to be ~ 10 KW which is in reasonable agreement with the applied ECRH power in the plug and anchor. (Note, the estimated ECRH power was reduced by the profile parameter K_1 to be consistent with the power balance.)

VI. Start-Up

Startup of the proposed machine entails the use of RF heating in the anchor and plug, programmed cold gas feed, and neutral beam injection. A possible startup scenario consists of the following sequence of events.

(1) The central cell density will be built up by using ECRH for preionization and by applying ICRH as a heat source which will elevate the ion temperature and maintain the electron temperature as the density exceeds microwave cut off. The cold gas feed into the central cell will be programmed so as to optimize the density build up.

(2) Simultaneous with the density build up in the central cell, the magnetically trapped hot electrons will be generated in the plugs and anchors. The loss of plasma from the central cell will provide a particle source for the hot electrons and a target plasma for the neutral beams. Additional trapping of the central cell stream can be accomplished by application of fundamental frequency ICRF as has been demonstrated on Phaedrus [23].

(3) Neutral beams will be started in the plugs and anchors, establishing the equilibrium hot ion axial density profile.

(4) ECRH is applied near the outer peak in the plug generating the confining potential for the central cell ions. (The heating of these "warm" electrons may occur simultaneously with the heating of the hot electrons (step 2)).

Each of the above steps in the startup phase will be discussed in more detail in the remainder of this section.

Governing Equations:

The governing particle and energy balance equations for the startup phase in the RF heated cells are the following:

$$\frac{dn}{dt} = n\left(n_o \langle\sigma v\rangle_i - \left(\frac{n}{n\tau}\right)\right) \tag{26}$$

$$\frac{dnT_e}{dt} = P_\mu - P_{ei} - \frac{n^2 T_e}{(n\tau)} - nn_o \varepsilon_i \langle\sigma v\rangle_i \tag{27}$$

$$\frac{dnT_i}{dt} = P_{HF} + P_{ei} - nT_i\left(n_o \langle\sigma v\rangle_{cx} + \frac{n}{(n\tau)}\right) \tag{28}$$

$$P_{ei} = 6.4 \times 10^{-8}\, n^2 (T_e - T_i)\, T_e^{-3/2} \tag{29}$$

In the above equations, n_o is the neutral density, $\langle\sigma v\rangle_i$ and $\langle\sigma v\rangle_{cx}$ are the ionization and charge exchange rates averaged over a Maxwellian, $(n\tau)$ is an appropriate density-confinement time (see below), P_{ei} is the power transfer due to electron-ion collisions, P_μ is the applied microwave ECRH power, and P_{HF} is the applied high frequency ICRH power and ε_i the energy expended per ionization event.

The particle balance [5] in the plug and anchor is

$$\frac{dn_h}{dt} = \left[\frac{(\langle\sigma v\rangle_i + \langle\sigma v\rangle_{cx}) n_t L_e}{v_b} \quad \frac{I_b}{e V_e}\right] + \left[\frac{\langle\sigma v\rangle_i n_n L_e}{v_b}\right] \quad \frac{I_b}{e V_e} - \frac{n_h^2}{(n_n\tau)} - n_h n_o \langle\sigma v\rangle_{cx}' . \tag{30}$$

In Eq. 30, n_h is the hot beam injected ion density, n_t is the cold target ion density, I_b and v_b are the beam current and velocity, V_e is the effective volume of the plug, L_e is the effective path length for the neutral beam, and the bracketed expressions are the fraction of the neutral beam trapped due to ionization and charge exchange off the cold target plasma,

and due to ionization from cold electrons associated with the hot ion buildup.

Central Cell

The density in the central cell will be built up using ECRH and ICRH providing filling of the plug and generating a target plasma for neutral beam injection. ECRH at $2\omega_{ce}$ will be used for preionization and to build up a low density (~ 3×10^{11} cm^{-3}), hot electron plasma (5 - 25 KeV). The microwave power and the neutral density gas feed will be adjusted to achieve these parameters. At this point, the neutral gas feed will be increased and ICRH power will be applied. The newly created cold electrons will be initially heated by electron drag on the minority of hot electrons and later by drag on the warm ions. The power transfer between the hot and cold electrons will replace the microwave power as the density rises above the microwave cut off. The parameters of the initial hot electron population will be optimized to maximize this power transfer process. ICRH will be used to control the ion temperature maintaining a moderate temperature so that collisional trapping of ions in the plug will build up a suitable neutral beam target. The determination of the precise microwave and high frequency power levels that are required for central cell startup await further analysis. However, comparison with the power levels on the EBT-S experiment suggests, P_{μ} ~ 40 KW and P_{HF} ~ 100 KW. Use of $2\omega_{ce}$ heating for breakdown also awaits testing on the Phaedrus tandem mirror.

Barrier Electrons

The ~ 20 KeV barrier electrons will be generated simulataneously with the central cell buildup. The particle source for these electrons will be provided by the loss of electrons from the central cell that trap in the plug. The 28 GHz microwave power will be adjusted to reach near equilibrium conditions for the varying central cell particle source.

Neutral Beam Injection into Plug

Eq. 30 is the governing particle balance for build up of neutral beams in the plug. Referring to Table 2, the spatially averaged equilibrium parameters can be estimated to be $n_t \sim 1.2 \times 10^{12}$ cm^{-3}, $n_h(\text{ave}) \sim 6 \times 10^{12}$cm^{-3}, and $(n\tau) \sim 1 \times 10^{11}$. Assuming n_o is negligible, Eq 30 yields $I_b L_e/V_e \sim 0.02$ for steady state. Using these values, only ~ 2/3 of the equilibrium density n_h can be achieved in 10 msec.

To accelerate the build up either the target density or the neutral beam current must be increased. By increasing the target density by a factor of 2 or 3, the equilibrium hot ion density can be reached in 8 and 5 msec respectively.

The target ion density can be controlled by adjusting the central cell ion temperature through application of ICRF and the central cell gas feed. An additional neutral beam module may be required for startup to vary I_b so as to have an additional control on n_h and n_t during startup. From Eqn. 30, one can also estimate the maximum tolerable neutral pressure such that the charge exchange time is long compared with the confinement time. For $n_o \langle\sigma v\rangle_{cx} < 0.1\ \tau^{-1}$, $n_o \lesssim 10^8$. A plasma blanket and/or a plasma curtain in the neutral beam line will be used to insure this value of

neutral pressure. After the sloshing ion axial density profile is established, ECRH heating at ω_{ce} will be used to heat warm electrons generating the confining potential for central cell ions.

VII Conclusions

We have presented a self-consistent design of a tandem mirror in which the ion confinement is axisymmetric and thereby not subject to resonant transport. Plugs containing thermal barriers generated by sloshing ions are formed in simple mirror cells. Plug micro-stability accrues both from the presence of the transition plasma which reduces the hole size and the sloshing-ion distribution which can self trap warm plasma. The sloshing-ion midplane density depression generates a partial thermal barrier and provides ECRH accessibility for generating a μ-trapped electron population for full thermal barrier operation.

The peak plug fields are generated by circular coils; an arrangement that is optimum for creating the high fields required in advanced applications. Access is excellent within the plug. Furthermore, for a fusing central cell all of the neutrons would be generated away from the quadrupole anchors.

We have also suggested a start up scenario that does not require use of stream guns. This procedure would help decouple the plasma from the end walls thereby reducing energy losses at early times in the discharge.

Acknowledgement.

The authors wish to thank Drs. J. R. Conrad (U.Wisc.) for the neutral beam design analysis, R. W. Klinkowstein (MIT) for aid in the magnet design and M. J. Gerver (MIT) for assistance in micro-stability analysis. Drs. D. E. Baldwin (LLNL) and B. G. Logan (LLNL) provided many many useful insights into this work. Additionally, T. Kaiser (LLNL) developed the TARA geometry ballooning mode code and obtained the MHD results presented herein. This work was performed under U.S. DOE Contract, number DE-AC02-78ET-51013.

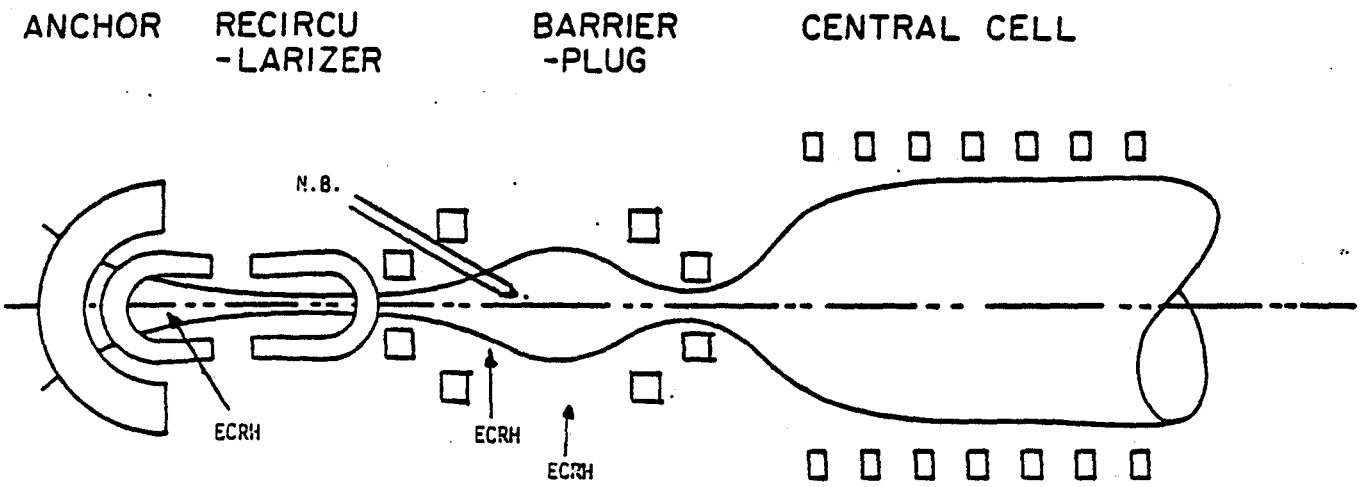
ANCHOR
RECIRCU
-LARIZER
BARRIER
-PLUG
CENTRAL CELL
N.B.
ECRH
ECRH
ECRH

Fig. 1

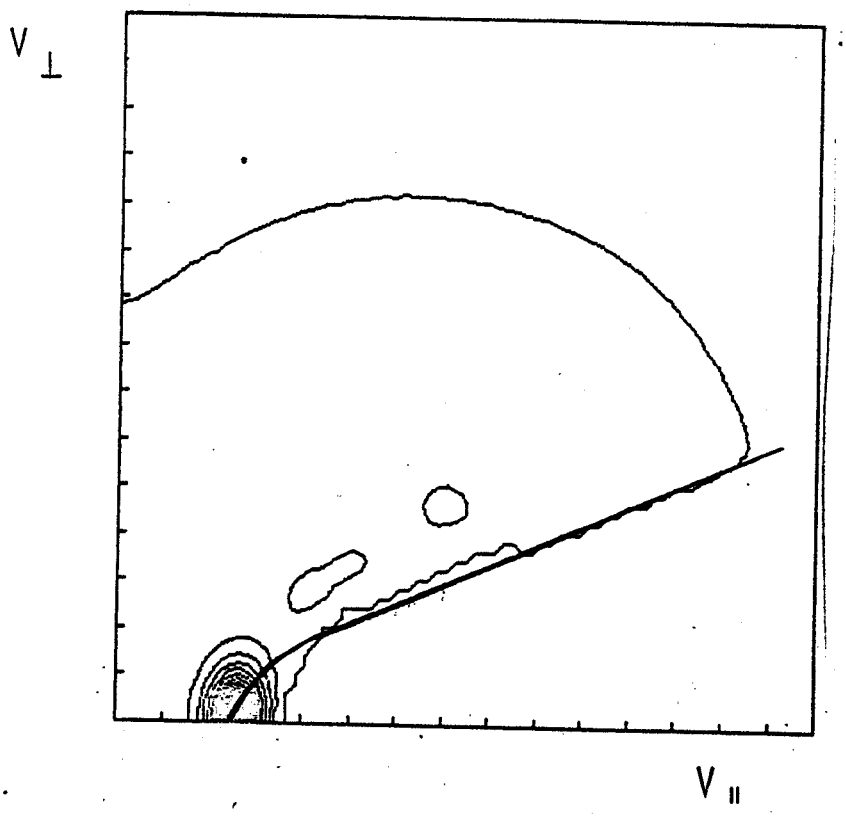

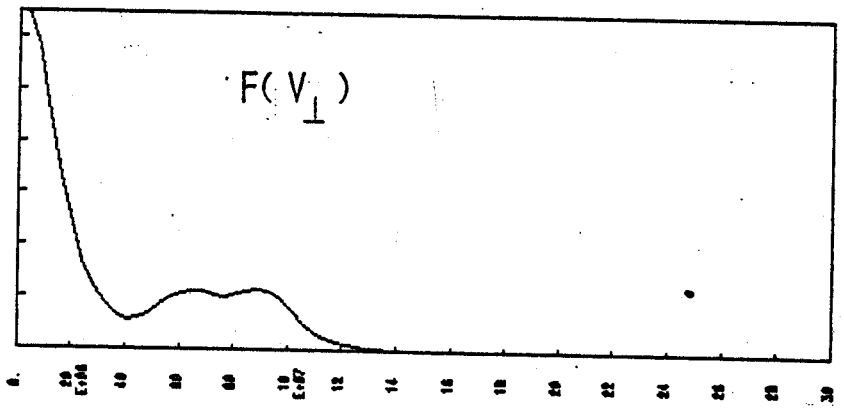

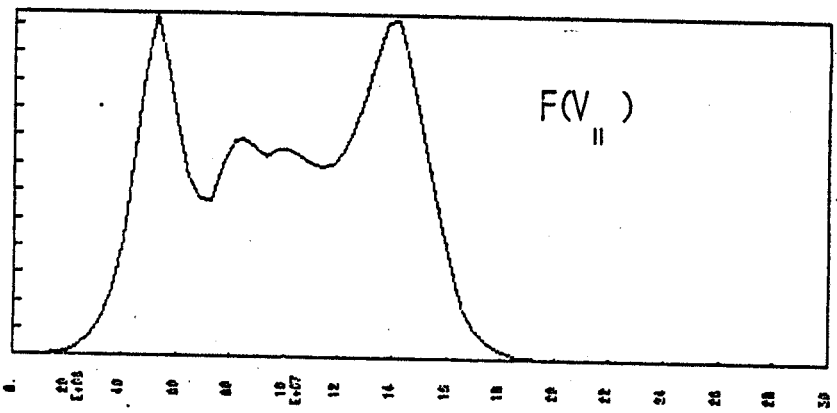

Fig. 2

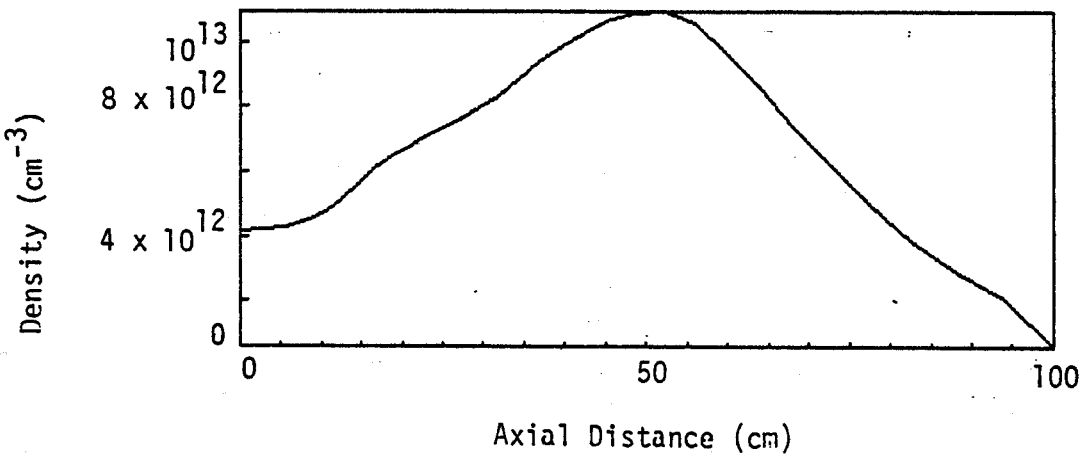
Density (cm^{-3})
10^{13}
8×10^{12}
4×10^{12}
0
0
50
100
Axial Distance (cm)

Fig. 3

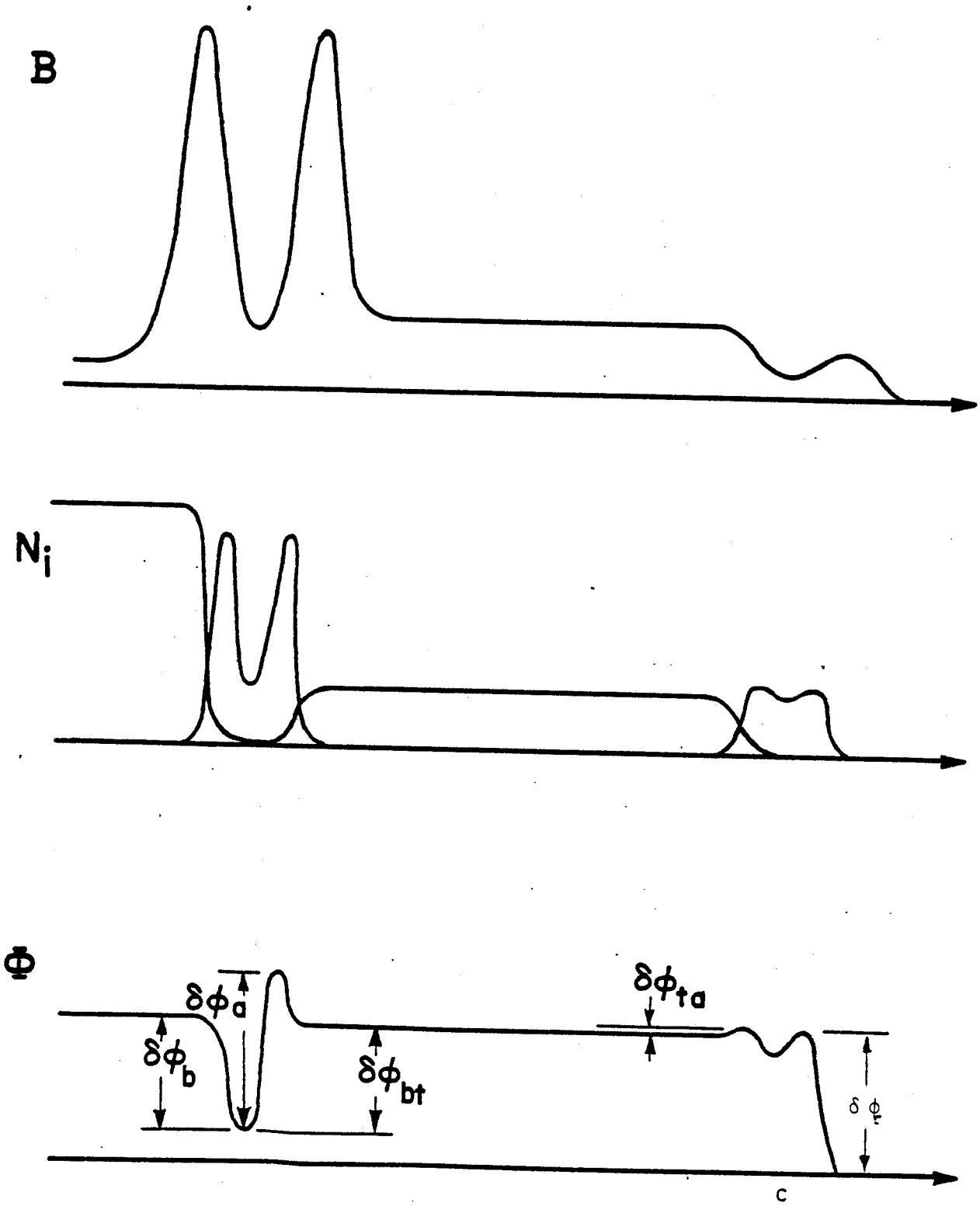
B
N_i
Φ
$\delta\phi_a$
$\delta\phi_b$
$\delta\phi_{bt}$
$\delta\phi_{ta}$
$\delta\phi_t$
c

Fig. 4

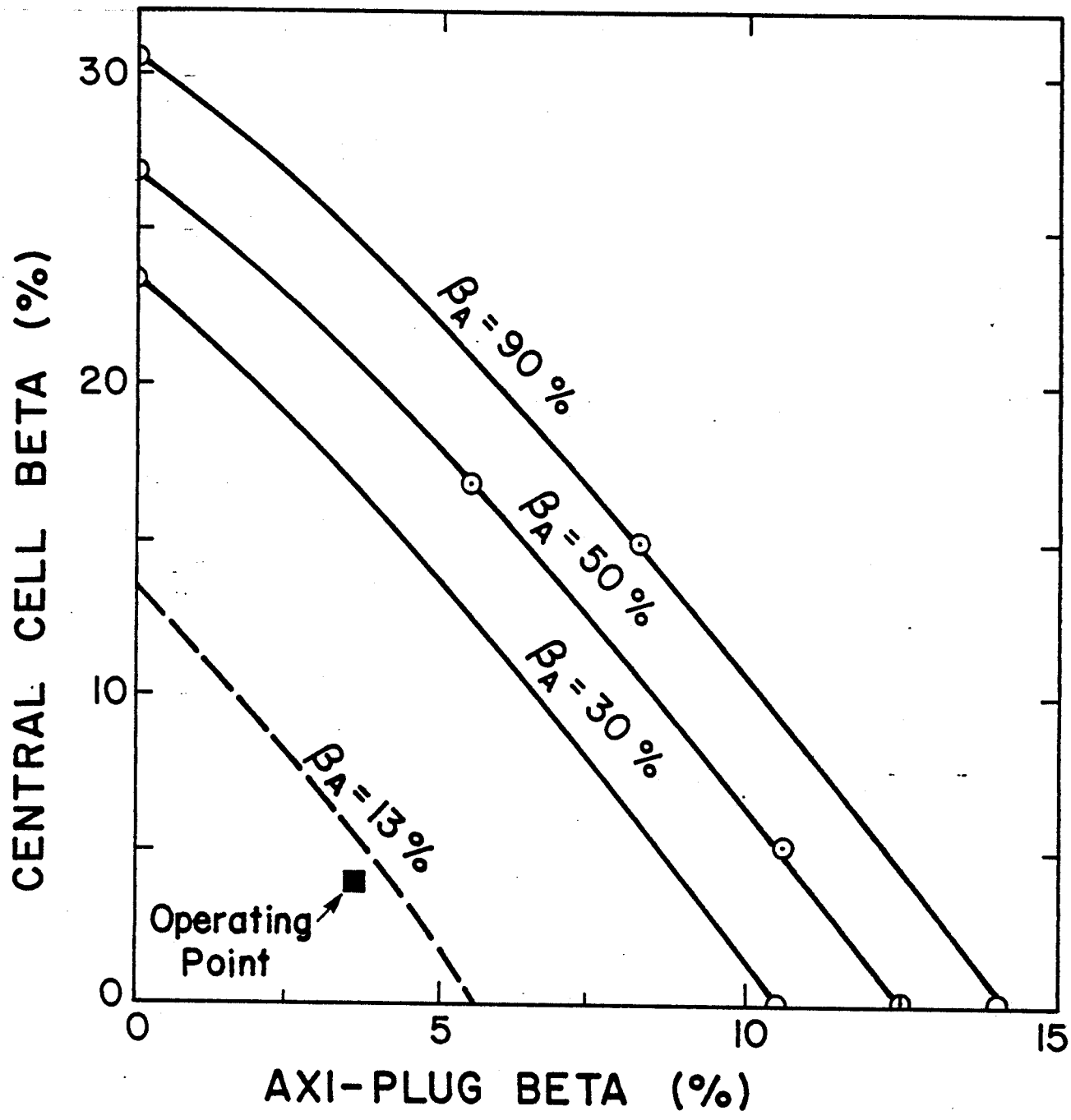
CENTRAL CELL BETA (%)
AXI-PLUG BETA (%)
0
10
20
30
0
5
10
15
β_A = 90 %
β_A = 50 %
β_A = 30 %
β_A = 13 %
Operating Point

Fig. 5

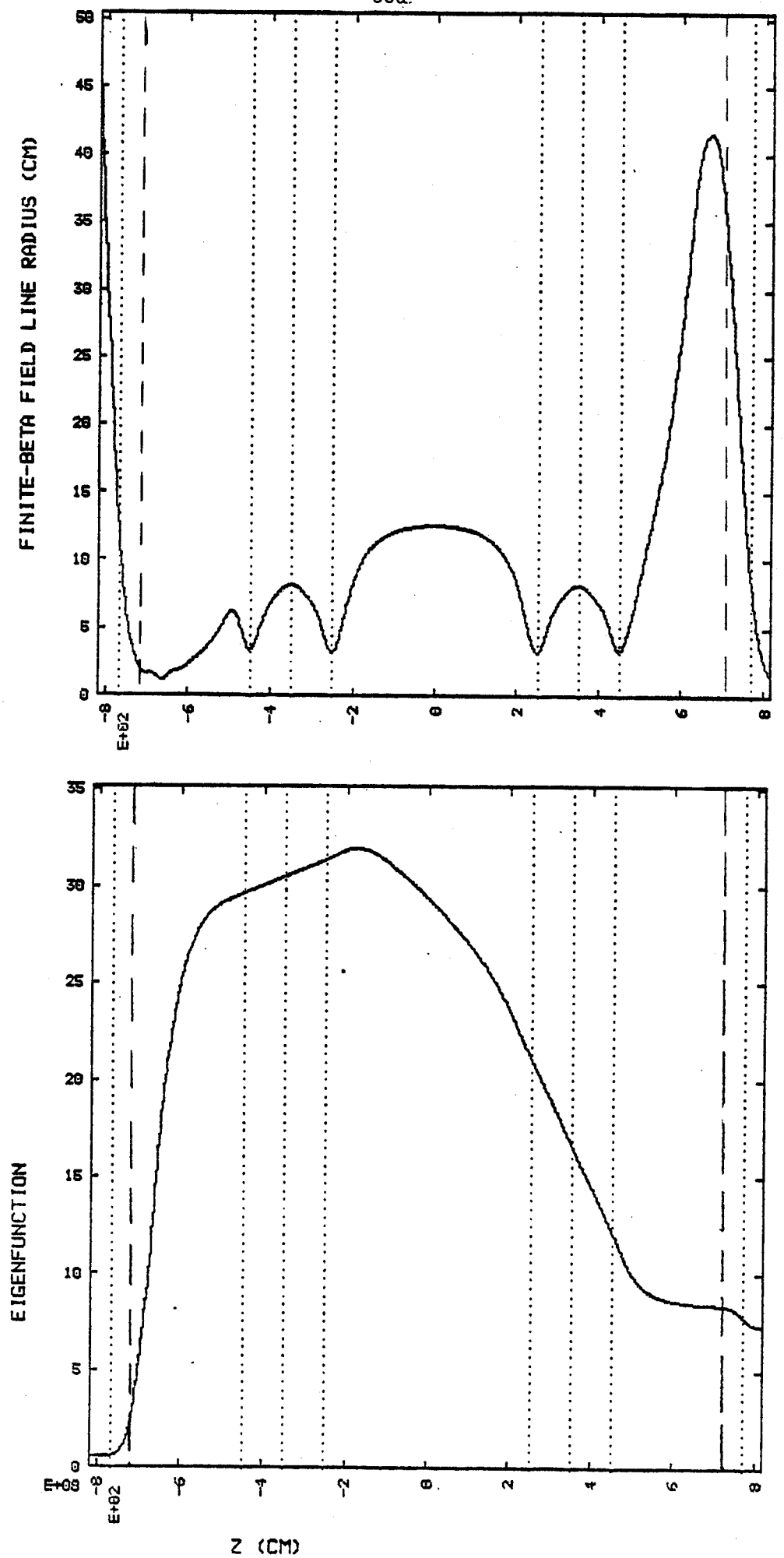
FINITE-BETA FIELD LINE RADIUS (CM)
50
45
40
35
30
25
20
15
10
5
0
-8
E+02
-6
-4
-2
0
2
4
6
8
EIGENFUNCTION
35
30
25
20
15
10
5
0
E+08
-8
E+02
-6
-4
-2
0
2
4
6
8
Z (CM)

Fig. 6

Figures

Fig. 1 - Schematic of coil set showing plasma boundary.

Fig. 2 - a) Velocity space contours and

b) f ($v_\perp$), f($v_\parallel$) for 35° injection into a mirror ratio = 6 cell.

Fig. 3 - Density Profile for 35° injection into a mirror ratio = 6 cell.

Fig. 4 - Magnetic Field, density and potential profiles with hot ion anchor.

Fig. 5 - Marginal stability boundary for MHD ballooning.

Fig. 6 - Field line radium and eigenfunction from Balloon Calculation.

Table 1

CENTRAL CELL PARAMETERS

L_c	5 m
r_c	12 cm
B_c	0.2 T
a_i	1.02 cm
N_c	4.0×10^{12} cm^{-3}
T_{ec}	400 eV
T_{ic}	400 eV
β_c	0.032
Azimuthal drift $\Delta\psi$	3.6
Collisionality $\nu_c t_{\parallel} = L_c/\text{mfp}$	0.013
Collisionality $(\nu_c t_{\parallel})\ (T_{ic}/\phi_c)\ (B_m/B_c)$	0.094
$n\tau_c$	2.6×10^{11} cm^{-3} - sec
Central Cell Volume	153 ℓ
Pastukhov Current	4.9 A/plug

TABLE 2

FOKKER-PLANCK RESULTS

$R = 6 \quad \theta_{LC} = 24^{\circ}$

$E_{INJ} = 15$ KEV

RUN	T31	T32	T36
θ_{INJ}	30°	35°	35°
$I_{INJ}(A)$	110	110	63
$N_C(CM^{-3})$	8.5×10^{12}	8.5×10^{12}	4×10^{12}
$N_B(CM^{-3})$	2.3×10^{12}	9.5×10^{12}	4.2×10^{12}
$N_A(CM^{-3})$	5.2×10^{12}	2.3×10^{13}	1.1×10^{13}
$N\tau(CM^{-3}\text{-SEC})$	3.4×10^{10}	1.2×10^{11}	1.0×10^{11}
$I_{CX}(A)$	2.4	9.5	2.2

Table 3

AXISYMMETRIC PLUG PARAMETERS

Neutral Beam Gaussian Half-Width	10 cm
Injection Angle	35°
Beam Energy	75% @ 15 KeV 15% @ 7.5 KeV 10% @ 5 KeV
Mirror Ratio of Well	6
Plasma Radius	7.5 cm
Plasma Length (mirror to mirror)	200 cm
Midplane density (N(b))	4.2×10^{12} cm^{-3}
Peak Density	1.1×10^{13} cm^{-3}
Peak Density Location ($B(Z)/B_o$)	2.4
$\delta\phi_a$	2.2 keV
$\delta\phi_b$	1.4 keV
Midplane Passing Density ($N_{ic}(b)$)	2.0×10^{11} cm^{-3}
Hot Ion Midplane Density ($N_{ih}(b)$)	3.0×10^{12} cm^{-3}
Passing + Trapped Cold Midplane Density	1.2×10^{12} cm^{-3}
g_b	6.0
T_{ew}	0.7 KeV
E_{eh}	12 KeV
Total Beam Current	63 A
$(N\tau)_p$	1.0×10^{11} cm^{-3}-sec
P_{ECRH} (warm electrons)	9.3 KW
P_{ECRH} (hot electrons)	2.0 KW
Plug Volume	22 ℓ

Table 4

Hot Ion Anchor Parameters

$\overline{E}_i$	12 keV
T_e	0.7 keV
n (midplane)	6×10^{12} cm^{-3}
B_o	4 KG
B_{max}	10 KG
B_c	5.2 KG
β_a	12%

Total neutral beam current injected 100A

TABLE 5

INPUT FOR FOKKER-PLANCK RUNS

Neutral Beam Energy	60% @ 20 keV 20% @ 10 keV 20% @ 6.67 keV
Ambipolar Potential (Midplane to Mirror Throat)	4.5 keV
Beam Footprint (full width to 1/e point)	$33/(\cos\theta_{inj})$cm along axis 9 cm perpendicular
Total Ionization Rate Coefficient 20, 10, 6.67, .005 keV	3.7×10^{-8}, 2.1×10^{-8}, 1.5×10^{-8}, 4.4×10^{-8} $cm^3/sec.$
Charge Exchange Rate Coefficient 20, 10, 6.67, .005 keV	6×10^{-8}, 4×10^{-8}, 6.6×10^{-7}, $1.2 \times 10^{-7} cm^3/sec.$
Beam Dispersion Along Axis	2.4°

TABLE 6

RESULTS OF FOKKER-PLANCK RUNS

Case Number	36	39	42	43
Injection Current (A)	200	100	100	100
Mirror Ratio	2	2.5	2.5	2.5
Neutral Density (cm^{-3})	1×10^{8}	1×10^{8}	1×10^{8}	3×10^{8}
Injection Angle	65°	65°	70°	65°
Midplane Density (cm^{-3})	2.2×10^{12}	6.1×10^{12}	1.2×10^{13}	6.1×10^{12}
Peak Density (cm^{-3})	4.0×10^{12}	9.2×10^{12}	1.5×10^{13}	6.8×10^{12}
Location Density Peak (cm)	20	16	12.5	18.6
Midplane Potential Depression (V)	390	273	164	69 ev
$n\tau$ (cm^{-3} - sec)	1.3×10^{10}	6.3×10^{10}	9.7×10^{10}	4.0×10^{10}

References

1. DIMOV, G.I., ZAKAIDAKOV, V.V., KISHINEVSKY, M.E., FIZ. Plasmy 2 (1976) 597.

2. FOWLER, T.K., LOGAN, B.G., COMM. on Plasma Phys. and Cont. Fus. 2 (1977) 167.

3. BALDWIN, D.E., LOGAN, B.G., Phys. Rev. Lett. (1979).

4. KESNER, J., Axisymmetric Sloshing Ion Tandem Mirror Plugs, U. Wisc. Rept. UWFDM-328 (1979), Nuc. Fus. 20 (1980) 557.

5. LOGAN, B.G., in "Physics Basis for MFTF-B," Lawrence Livermore Laboratory rept. UCID-18496, (1980).

6. LAUNOIS, D., LECOUSTEY, P., TACHON, J., KESNER, J., CHATALLIER, M., Nuc. Fus. 12 (1972) 673. See also LAUNOIS, D., LECOUSTEY, P., TACHON, J., KESNER, J., NICHOLAS, N., Plasma Phys. and Cont. Nuc. Fus. Res. (Proc. 4th Int. Conf., Madison), 2 IAEA Vienna (1971) 575.

7. KESNER, J., Plasma Physics 15 (1973) 577.

8. R. S. Post, J. Kesner, "Construction of Tara Tandem Mirror Facility," Proposal submitted to DOE, Nov. 1980.

9. KESNER, J., Tandem Mirror Sloshing Electron Plugs, Nuc. Fus. 21 (1981) 97.

10. HASTE, G. R. and LAZAR, N. H., Phys. Fluids 16 (1973) 683, Ard, W. B. et al., Plasma Phys. and Cont. Nuc. Fus. Res. (proc. 4th Int. Conf., Madison), 2 IAEA Vienna (1971) 619.

11. COENSGEN, F. H., SIMONEN, T. C., CHARGIN, A. K., LOGAN, B. G., TMX Upgrade Major Project Proposal, Lawrence Livermore Laboratory Rept. LLL-Prop-172 (1980).

12. CUTLER, T. A., PEARLSTEIN, L. D., RENSINK, M. E., LLL Rept. UCRL-52233 (1977).

13. CUTLER, T. in "Physics Basis of MFTF-B", op. cit. 5.

14. COHEN, R. H., BERNSTEIN, J. B., DORNING, J. J., ROWLANDS, G., Lawrence Livermore Laboratory Rept. UCRL-84147 (1980).

15. KESNER, J., KNORR, G., NICHOLSON, D.R., "Self Consistent Potential Variations in Magnetic Wells," U. of Iowa Rept. 80-11 (1980).

16. COHEN, R. H., "Ambipolar Potential Profiles in Thermal-Barrier Cells," LLNL Rept. UCRL-84535 (1980).

17. BALDWIN, D. E. et. al., Plasma Physics and Cont. Nuc. Fus. Res. [Proc. 8th Int. Conf., Brussels] (1980).

18. BALDWIN, D. E. and JONG, R. A., Phys. Fluids 22, 119 (1979).

19. KESNER, J., Comm. on Plasma Physics and Cont. Fus.

20. KAISER, T. B., Bull. APA 23, 754 (1978), see also "Physics Basis of MFTF-B" IV-B, LLNL Rept. UCID-18496-2 (1980) IV-43.

21. HOSEA, J. C. and SINCLAIR, R. M., Phys. Fluids 13, 701 (1970)

22. BREUN, R., CONRAD, J. R., GOLOVATO, S., KESNER, J., POST, R. S., et. al., Proc. 8th Int. Conf. on Cont. Fus., IAEA, Brussels (1980). See also SMITH, D.K., Ph.D. Thesis, Univ. of Wisc., 1980.

23. McVEY, B. D., and Phaedrus group, private com.